

Raman, electron microscopy and electrical transport studies of x-ray amorphous Zn-Ir-O thin films deposited by reactive DC magnetron sputtering

This content has been downloaded from IOPscience. Please scroll down to see the full text.

2015 IOP Conf. Ser.: Mater. Sci. Eng. 77 012035

(<http://iopscience.iop.org/1757-899X/77/1/012035>)

View [the table of contents for this issue](#), or go to the [journal homepage](#) for more

Download details:

IP Address: 213.175.108.33

This content was downloaded on 07/05/2015 at 09:47

Please note that [terms and conditions apply](#).

Raman, electron microscopy and electrical transport studies of x-ray amorphous Zn-Ir-O thin films deposited by reactive DC magnetron sputtering

M. Zubkins, R. Kalendarev, J. Gabrusenoks, K. Smits, K. Kundzins, K. Vilnis, A. Azens, J. Purans

Institute of Solid State Physics, University of Latvia, Riga, Latvia

E-mail: zubkins@cfi.lu.lv

Abstract. Zn-Ir-O thin films on glass and Ti substrates were deposited by reactive DC magnetron sputtering at room temperature. Structural and electrical properties were investigated as a function of iridium concentration in the films. Raman spectrum of Zn-Ir-O (61.5 at.% Ir) resembles the spectrum of rutile IrO_2 , without any distinct features of wurtzite ZnO structure. SEM images indicated that morphology of the films surface improves with the iridium content. EDX spectroscopy and cross-section SEM images revealed that the films growing process is homogeneous. Crystallites with approximately 2 - 5 nm size were discovered in the TEM images. Thermally activated conductivity related to the variable range hopping changes to the non-thermally activated before iridium concentration reaches the 45 at.%.

1. Introduction

One of the obstacles to further developments of transparent electronics based on transparent conductive oxide (TCO) thin films is lack of p-type conductors [1]. Thin films with delafossite crystal structure (AMO_2) based on Cu are the most widely studied p-TCO material, but it suffers from low conductivity mainly due to low hole mobility [2]. In addition, elevated substrate temperature, which is required for thin film deposition [3], is not suitable for deposition on polymer substrates. From other p-TCO alternatives, such as binary oxides (ZnO:N , /As, /P, NiO [4]), mixed oxides ($\text{In}_2\text{O}_3\text{-Ag}_2\text{O}$ [5]) or spinels (ZnIr_2O_4 [6], NiCo_2O_4 [7]), the amorphous thin films (Zn-Rh-O [8], Zn-Ir-O [9]) gained much interest due to low deposition temperature. No long range order is required for p-type conductivity in these materials and therefore the conductivity is independent of the film structure.

Earlier study [10] confirmed that the Zn-Ir-O films deposited by reactive DC magnetron sputtering do not show any observable XRD peak features, indicating that these films are x-ray amorphous. Electrical resistivity and transmittance of the films decreases considerably with the iridium content.

Magnetron sputtering is a widely used technique for thin film deposition, providing a high degree of composition control even for complex compound films. For binary metal oxides, either varied target composition or co-sputtering of two metal targets can be used to vary the metal-to-metal ratio in the films. The stoichiometry with respect to oxygen can be varied by varying the partial pressure of oxygen in the sputtering atmosphere.



This paper reports on properties of x-ray amorphous Zn-Ir-O thin films deposited by reactive DC magnetron sputtering. Structural and electrical properties were studied by Raman technique, SEM, TEM, EDX and DC conductivity measurements as a function of temperature.

2. Experimental details

Zn-Ir-O thin films were deposited on glass and Ti substrates, coated simultaneously by reactive DC magnetron sputtering from a metallic Zn (99.95 wt %) target with Ir (99.6 wt %) pieces on the target surface in an Ar+O₂ atmosphere. The substrates were washed in acetone and distilled water before deposition. Vacuum chamber was pumped to base pressure below 1×10^{-5} Torr by a turbo-molecular pump. During the deposition the substrate was kept at room temperature, the sputtering was conducted at 10 mTorr working pressure and 100 W sputtering power. The target to substrate distance was 5 cm. A set of samples was deposited at different oxygen to argon gas ratios (1/4, 1/2/, 1/1) and at different fractions of iridium on the zinc target erosion zone (1, 3, 5, 7, 10, 13, 15 %) to vary the atomic composition in the films. Pure c-ZnO_x and a-IrO_{2-x} thin films were deposited as a reference samples.

Elemental analysis of Zn-Ir-O films was done by X-ray fluorescence spectrometer Eagle III. The Raman shift from pulsed YAG laser (532 nm) was measured to further identify the structure of Zn-Ir-O thin films. Backscattering geometry was used to collect Raman spectra. Microstructural information on selected samples was obtained by high resolution scanning and transmission electron microscopy (SEM:Tescan Lyra and TEM: Tecnai GF20). The powder-like TEM samples were prepared by mechanical scraping from glass substrates. The electrical resistivity as a function of temperature was determined by Hall effect measurement system HMS 5000.

3. Results and discussion

3.1. Zn-Ir-O structural analysis

Normalized Raman spectra of Zn-Ir-O (6.7, 16.0, 24.1, 61.5 at.% Ir), x-ray amorphous iridium oxide (a-IrO_{2-x}) and crystalline zinc oxide (c-ZnO_x) films are shown in Fig. 1. Dashed vertical lines in Fig. 1 show the positions of the characteristic peaks of crystalline IrO₂ (rutile) and ZnO

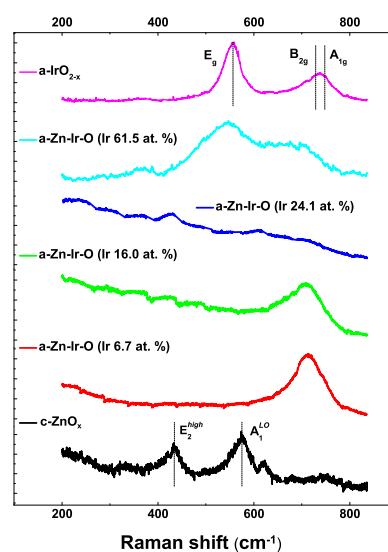


Figure 1. Raman spectra of Zn-Ir-O (6.7, 16.0, 24.1, 61.5 at.% Ir), a-IrO_{2-x} and c-ZnO_x.

(wurzite) [11,12]. Experimental configuration allows to detect only E_2^{high} and A_1^{LO} in ZnO case. In the Raman spectrum of Zn-Ir-O (6.7 at.% Ir) a band at 712 cm^{-1} is well observed. Intensity of this band decreases with the iridium concentration and disappears before concentration reaches 24.1 at.%. It is possible that this band corresponds to any solid solution of Zn and Ir oxides (for example Zn_2IrO_4 or Ir_2ZnO_4). We are not aware of any Raman spectra for these compounds available in the literature. Though Raman spectrum of similar compound Zn_2SnO_4 have strong A_g symmetry band at 668 cm^{-1} , with other Raman active bands being of low intensity [13]. Our ab initio calculation of lattice vibrations for crystalline Zn_2IrO_4 gives high frequency A_g vibration at 601 cm^{-1} . Raman spectrum of Zn-Ir-O (61.5 at.% Ir) mainly consists of IrO_2 phase and resembles the spectrum of a-IrO_{2-x} , without any distinct features of wurtzite ZnO. Due to amorphous Zn-Ir-O structure Raman peaks are extremely wide. The absolute intensity of c-ZnO_x spectrum is significantly lower compared to a-IrO_{2-x} spectrum, therefore, Raman data does not allow to draw definite conclusions about the presence or absence of ZnO phase in the films. Again, to our knowledge, there is no Raman literature data of amorphous ZnO thin films to compare with.

Zn-Ir-O thin films with low iridium concentration (6.7 at.%) have approximately 100 - 200 nm large particles on the surface (Fig. 2(a)). The cross-section SEM images of this film revealed that the bottom surface contains nano-sized holes of approximately 150 nm diameter (Fig. 2(d)).

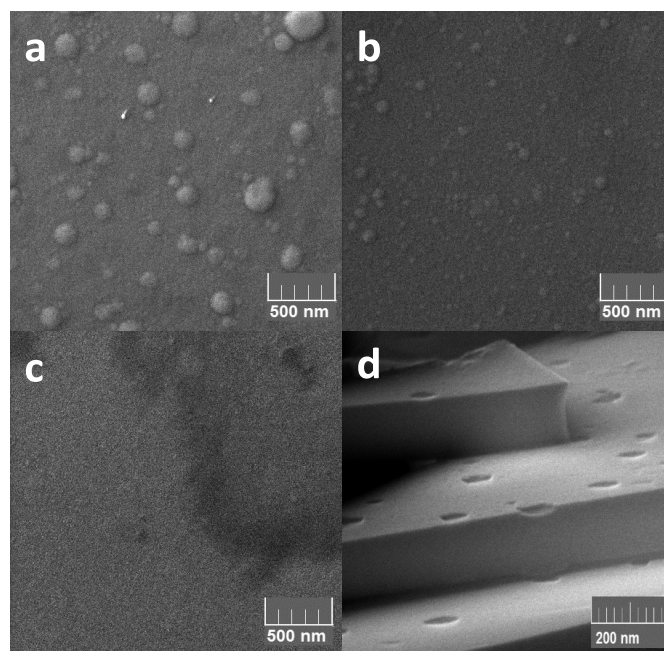


Figure 2. SEM images of Zn-Ir-O (6.7(a), 24.1(b), 40.6(c) at.% Ir and cross-section of 6.7(d) at.% Ir.

It could be speculated that the holes may be related to the way the islands grow and coalesce on the substrate in the beginning of the deposition. Size and concentration of the particles decreases with the amount of iridium (Fig 2(b)) and disappears before the iridium concentration reaches 40 at.% (Fig. 2(c)).

Fig. 3(a,b) shows the TEM images of the Zn-Ir-O (6.7, 67.4 at.% Ir) thin films. Atomic

rows observed in the TEM images indicate that all the Zn-Ir-O thin films contain randomly oriented crystallites with approximately 2 - 5 nm size. These nucleation centers do not grow large enough to fill the whole volume of the film, amorphous atomic network is still observed around the nano-crystallites.

200 nm distance of the samples was scanned by energy dispersive x-ray spectroscopy (EDX). EDX results indicate that all the elements (Zn, Ir, O) are distributed uniformly across the film.

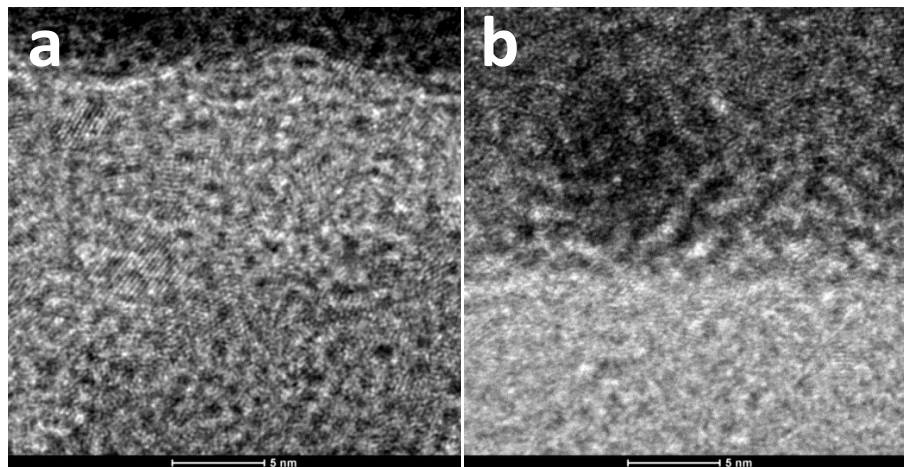


Figure 3. TEM images of Zn-Ir-O (6.7(a), 67.4(b) at.% Ir) thin films.

3.2. Zn-Ir-O electrical properties

The electrical transport properties of the samples were investigated by measuring the DC conductivity as a function of temperature between 90 K and 330 K. Fig 4(a) shows the $\ln \rho$ as a function of $1000/T$ (K^{-1}) and T (K). Since the experimental data do not have linear behaviour against $1000/T$ axis, the experimental data cannot be fitted by the general conduction activation mechanism $\rho(T) = \rho_0 \exp\left(-\frac{E_a}{k_B T}\right)$, which is commonly used to characterize the band conduction for semiconductors. Hopping conduction is one of the major features exhibited by

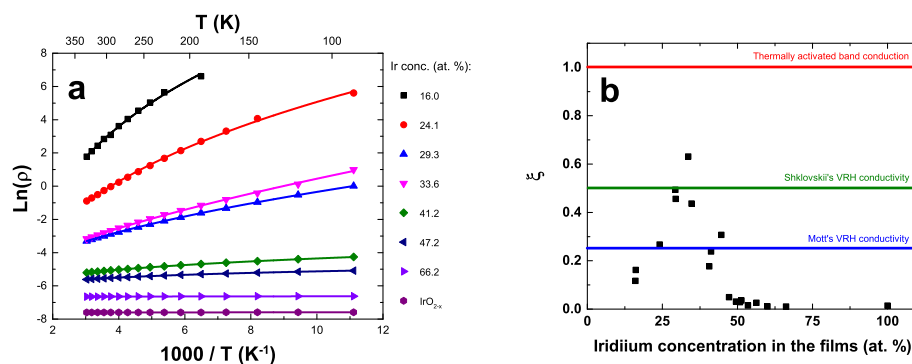


Figure 4. $\ln \rho$ as a function of $1000/T$ (K^{-1}) and T (K) (a), and ξ as a function of iridium concentration in the films (b).

semiconductors with disorder structure [14] and this mechanism of conductivity is widely used for the interpretation of the experimental data. Generally, temperature dependence of the resistivity is given by $\rho(T) = \rho_0 \exp\left(-\frac{T_0}{T}\right)^\xi$. Value of ξ depends on the model of conductivity ($\xi=1/4$ Mott's variable range hopping (VRH) without Coulomb interaction [14], $\xi=1/2$ Shklovskii's VRH with long range electron-electron Coulomb interaction [15] and $\xi=1$ thermally activated band conduction). The movement of the charge carriers in electric field in the hopping conductivity is realized as tunnelling transitions with absorption or emission of phonons within a narrow strip of the localized states in the vicinity of the Fermi level. The solid lines in Fig. 4(a) are the theoretical fitting to the experimental data according to $\ln\rho=a+bT^\xi$, where a , b and ξ are fitting parameters. Exponent ξ from the fits to the experimental data of all samples as a function of iridium concentration is shown in Fig. 4(b). Zn-Ir-O thin films with the iridium concentration in the range from 0 to 16 at.% are not conductive. A thermal activated transport is found in the 16 – 45 at.% iridium concentration range indicating semiconductor behaviour. Values of ξ indicate that this thermal activated transport is related to the VRH. The almost constant resistivity i.e. not thermally activated conductivity is observed in the 45 – 100 at.% iridium concentration range.

4. Conclusions

Based on SEM and EDX studies, x-ray amorphous Zn-Ir-O thin films deposited by reactive DC magnetron sputtering are homogeneous in composition. However, high resolution TEM images revealed that structure contains randomly oriented nano-crystallites with approximately 2 - 5 nm size. Raman studies indicate that nano-crystallites are related to the IrO₂ phase at high iridium concentration (61.5 at.%). Phase of nano-crystallites at low iridium concentration has not been established.

Thermally activated variable range hopping is the dominated electrical mechanism in the Zn-Ir-O thin films with the iridium concentration from 16 to 45 at.%. Further increase of iridium content changes the electrical mechanism to the non-thermally activated conductivity.

Acknowledgments

This work has been supported by VBBKC L-KC-11-0005 project Nr.KC/2.1.2.1.1/10/01/006,5.3

References

- [1] Szyszka B, Dewald W, Gurram S K, Pflug A, Schulz C, Siemers M, Sittinger V and Ulrich S 2012 Current Applied Physics 12 S2-S11
- [2] Tate J, Jayaraj M K, Draeseke A D, Ulbrich T, Sleight A W, Vanaja K A, Nagarajan R, Wager J F and Hoffman R L 2002 Thin Solid Films 411 119-124
- [3] Banerjee A N and Chattopadhyay K K 2005 Progress in Crystal Growth and Characterization of Materials 50 52-105
- [4] Sato H, Minami T, Takata S and Yamada T 1993 Thin Solid Films 236 27
- [5] Minami T, Shimokawa K and Miyata T 1998 J. Vac. Sci. Technol. A 16 1218
- [6] Dekkers M, Rijnders G and Blank D G A 2007 Appl. Phys. Lett. 90 021903
- [7] Windisch Jr. C F, Ferris K M and Exarhos G J 2001 J. Vac. Sci. Technol. A 19 1647
- [8] Narushima S, Mizoguchi H, Shimizu K I, Ueda K, Ohta H, Hirano M, Kamiya T and Hosono H 2003 Advanced Materials 15 (17) 1409-1413
- [9] Dekkers M 2007 Ph. D. Thesis, University of Twente, Enschede p. 113
- [10] Zubkins M, Kalendarev R, Gabrusenoks J, Vilnis K, Azens A and Purans J 2014 Phys. Status Solidi C 11 (9) 1493-1496
- [11] Korotcov A V, Huang Y S, Tiong K K and Tsai D S 2007 J. Raman Spectrosc. 38 737
- [12] Khan A 2010 J. Pak. Mater. Soc. 4(1) 5
- [13] Shen X, Shen J. and You S. J. 2009 J. Appl. Phys. 106, 113523
- [14] Mott N F 1968 J. Non-Crys. Solids 1 1
- [15] Efros A L and Shklovskii B I 1975 J. Phys. C. 8 L49